⌘ *Author's Choice*

THE JOURNAL OF BIOLOGICAL CHEMISTRY VOL. 284, NO. 39, pp. 26447–26455, September 25, 2009

Thyrotropin Receptor Activation Increases Hyaluronan Production in Preadipocyte Fibroblasts

*CONTRIBUTORY ROLE IN HYALURONAN ACCUMULATION IN THYROID DYSFUNCTION**

Received for publication, April 3, 2009, and in revised form, June 24, 2009 Published, JBC Papers in Press, July 24, 2009, DOI 10.1074/jbc.M109.003616

Lei Zhang[‡], Timothy Bowen[§], Fiona Grennan-Jones[‡], Carol Paddon[‡], Peter Giles[¶], Jason Webber[§], Robert Steadman[§], and Marian Ludgate[‡1]

From the [‡]Centre for Endocrine & Diabetes Sciences, the [§]Institute of Nephrology, and the [¶]Biostatistics & Bioinformatics Unit, School of Medicine, Cardiff University, Cardiff CF14 4XN, United Kingdom

The thyrotropin receptor (TSHR) is expressed during lineage-specific differentiation (*e.g.* adipogenesis) and is activated by TSH, thyroid-stimulating antibodies, and gain-of-function mutations (TSHR*). Comparison of gene expression profiles of nonmodified human preadipocytes ($n = 4$) with the parallel TSHR* population revealed significant up-regulation of 27 genes including hyaluronan (HA) synthases (HAS) 1 and 2. The array data were confirmed by quantitative PCR of HAS1 and HAS2 and enzyme-linked immunosorbent assay measurement of HA; all values were significantly increased ($p < 0.03$) in TSHR*-expressing preadipocytes ($n = 10$). Preadipocytes ($n = 8$) treated with dibutyryl (db)-cAMP display significantly increased HAS1 and HAS2 transcripts, HAS2 protein, and HA production ($p < 0.02$). HAS1 or HAS2 small interfering RNA treatment of db-cAMP-stimulated preadipocytes ($n = 4$) produced 80% knockdown in HAS1 or 61% knockdown in HAS2 transcripts (compared with scrambled), respectively; the corresponding HA production was reduced by 49 or 38%. Reporter assays using A293 cells transfected with HAS1 promoter-driven plasmids containing or not containing the proximal CRE and treated with db-cAMP revealed that it is functional. Chromatin immunoprecipitation, using a cAMP-responsive element-binding protein antibody, of db-cAMP-treated preadipocytes ($n = 4$) yielded products for HAS1 and HAS2 with relative fold increases of 3.3 ± 0.8 and 2.6 ± 0.9, respectively. HA accumulates in adipose/connective tissues of patients with thyroid dysfunction. We investigated the contributions of TSH and thyroid-stimulating antibodies and obtained small (9–24%) but significant ($p < 0.02$) increases in preadipocyte HA production with both ligands. Similar results were obtained with a TSHR monoclonal antibody lacking biological activity ($p < 0.05$). We conclude that TSHR activation is implicated in HA production in preadipocytes, which, along with thyroid hormone level variation, explains the HA overproduction in thyroid dysfunction.

The thyrotropin receptor (TSHR)[2] is a G-protein-coupled receptor, which, in addition to its well characterized role in controlling thyrocyte function and growth (1), has been shown to be up-regulated during lineage-specific differentiation of adult precursors found in bone marrow and adipose tissue, *e.g.* preadipocyte adipogenesis to mature fat cells (2, 3). To investigate a potential role in these tissues, we performed microarray analyses of human preadipocytes transduced with a gain-of-function mutant TSHR and the equivalent nonmodified populations. Hyaluronan synthases 1 and 2 (HAS1 and HAS2) are two of the three synthases that produce hyaluronan (HA) and were among a small number of genes whose expression was significantly increased in the mutant TSHR population.

HA is a ubiquitous linear polysaccharide component of the extracellular matrix, which influences cellular proliferation and migration following injury and plays an important biological role in tissue remodeling, wound healing, and the phenotypic transformation of cells (4). HA occupies a large hydrodynamic volume acting as a lubricant, support, and cushion in different tissues. It is synthesized on the inner surface of the plasma membrane and extruded to the extracellular matrix by three differentially regulated HAS enzymes about the control of which very little is known (5). HAS1 has a tissue-specific expression, being present, for example, in dermal fibroblasts but absent in oral mucosal fibroblasts (6); HAS2 is inducible, and HAS3 is constitutively expressed in most cell types.

The skin and adipose/connective tissue of individuals with thyroid dysfunction accumulate glycosaminoglycans (GAG), predominantly HA (7). HA is hydrophilic and thus generates the widespread build-up of mucopolysaccharide that produces edema in hypothyroidism. In contrast, the deposition of HA is assumed to be more localized in hyperthyroid conditions such as Graves disease (GD) in which the orbital and pretibial regions are the most affected and can result in Graves ophthalmopathy (GO) and pretibial myxoedema, respectively (8). The major cause of thyroid dysfunction is autoimmunity, and several immunomodulators, *e.g.* interleukin-1 and transforming growth factor β (both macrophage products), can induce/enhance HA production *in vitro* (9, 10). Furthermore, serum IgG from patients with GD can induce hyaluronan production in cultured GD (but not normal) fibroblasts. The effect appears to

* This work was supported by a grant from the Wellcome Trust.

⌘ *Author's Choice*—Final version full access.

[1] To whom correspondence should be addressed. Tel.: 44-2920-745457; Fax 44-2920-744671; E-mail: ludgate@cf.ac.uk.

[2] The abbreviations used are: TSHR, thyrotropin receptor; TSAB, thyroid-stimulating antibodies; mAb, monoclonal antibody; HA, hyaluronan; HAS, HA synthase(s); QPCR, quantitative PCR; ELISA, enzyme-linked immunosorbent assay; siRNA, small interfering RNA; db, dibutyryl cAMP; CRE, cAMP-responsive element; CREB, CRE-binding protein; GAG, glycosaminoglycan(s); GD, Graves disease; GO, Graves ophthalmopathy; CM, complete medium; ChIP, chromatin immunoprecipitation; TCN, transcript copy numbers; APRT, adenosine phosphoribosyl transferase.

TABLE 1
PCR primers used indicating exon location and size of amplicon

	Forward primer	Reverse primer
hAPRT (247 bp)	GCTGCGTGCTCATCCGAAAG (exon 3)	CCTTAAGCGAGGTCAGCTCC (exon 5)
hHAS-1 (375 bp)	AAGGCGCTCGGAGATTCGGTGGACT (exon 2)	GCTGAGCATGCGGTTGGTGAGGTG (exon 4)
hHAS-2 (362 bp)	CTGGGACGAAGTGTGGATTATGTA (exon 2)	ACCCGGTTCGTGAGATGC (exon 4)
hHAS-3 (417 bp)	CTCGGCCCAGCGCATCTCCTT (exon 2)	ACATCTCCCCCGACTCCCCCTACT (exon 3)

be mediated by the receptor for IGF-1 and related activating antibodies (11).

Activation of the TSHR occurs in most patients with thyroid dysfunction through thyroid-stimulating antibodies (TSAB) in hyperthyroid GD or elevated TSH in hypothyroidism. In light of our array data, we hypothesize that TSAB or supraphysiological TSH target and activate the TSHR and stimulate the overproduction of HA. We report our findings on HA production in response to activation and/or cross-linking of the TSHR achieved using ligands and gain-of-function TSHR mutations naturally occurring in toxic adenoma and familial hyperthyroidism (reviewed in Ref. 12).

EXPERIMENTAL PROCEDURES

All of the reagents were obtained from Sigma-Aldrich, and tissue culture components were from Cambrex unless otherwise stated.

Adipose Tissue Collection and Preparation—Adipose tissue was collected with informed consent and local research ethics committee approval from several depots: orbit (n = 12, 9 patients with GO all undergoing decompressive surgery and having inactive disease with a clinical activity score below 2) and nonorbit (n = 11, predominantly subcutaneous from patients undergoing elective open abdominal surgery for nonmetabolic conditions).

Orbital preadipocytes were obtained from adipose tissue explants,, and nonorbital preadipocytes were obtained by collagenase digest, both as previously described (13). Preadipocytes were cultured in Dulbecco's modified Eagle's medium/Ham's F-12 10% fetal calf serum (complete medium (CM)) and were used at low passage number (<6); hence not all samples were analyzed in all experiments.

Generation of Populations for Gene Expression Profiling and Microarray Analysis—Activating mutant TSHR (L629F) was introduced into the various preadipocyte populations using retroviral vectors, previously produced in our laboratory (14). Geneticin selection resulted in mixed populations stably expressing the various TSHR, which exhibit increased basal levels of cAMP compared with the equivalent nonmodified cell population, all as previously described (13).

The nonmodified and mutant TSHR preadipocyte populations from four different individuals were cultured in CM in 10-cm Petri dishes until 90% confluent. RNA was then extracted from the cells using TRIzol reagent, according to the manufacturer's instructions. RNA quality was verified using an Agilent bioanalyzer prior to cDNA synthesis and *in vitro* transcription. The resulting cRNA was hybridized to Affymetrix HG-U133A chips, and the data were analyzed using Affymetrix MAS 5.0 software. Following successful QC analysis, the data were analyzed to identify differentially expressed genes using an unpaired Bayesian t test (15) with a false detection rate correction (16) for multiple testing. For visualization, the data were log-transformed and median-centered before hierarchical clustering and heat map visualization.

Strategies to Activate the TSHR and/or Increase cAMP—The expression of gain-of-function TSHR mutation provided one method. Alternatively, $\sim 5 \times 10^4$ nonmodified preadipocytes were plated in 6-well plates or 60-mm dishes in CM, and when they reached 70–80% confluence were serum-starved for 24 h and then treated for 4 or 24 h with 10^{-3} M dibutyryl cAMP (db-cAMP). Nonmodified preadipocytes in CM were also treated for varying time periods with 1–10 milliunits/ml TSH; 1 μg/ml monoclonal TSAB (IRISAB 2*); 1 μg/ml TSHR monoclonal antibodies lacking bioactivity (3G4 and BA8*); and 1 μg/ml monoclonal antibody to human thyroid peroxidase (mAb 47).

QPCR of HAS1/2/3 Genes—The various cell populations were plated in 6-well plates in CM, RNA was extracted following the various treatments, and 1 μg was reverse transcribed using standard protocols for QPCR analysis. Primers for the three HAS subtypes were designed using DNASTAR software to span intron-exon boundaries; details are provided in Table 1. To generate plasmid standards, PCR fragments were subcloned into pGEM-T (Promega) according to the manufacturer's instructions, and the plasmid identity was confirmed by sequencing. QPCR was conducted using SYBR Green incorporation measured on a Stratagene MX 3000. Each reaction comprised 1 μl of plasmid standard containing 10^6 to 10^2 copies, in a total volume of 25 μl. Initially the optimal primer combination, to generate a homogeneous amplification peak in the absence of primer dimers, was determined for each subtype.

QPCR measurement of HAS1/2/3 transcripts in the samples used 1 μl of cDNA (of a 20-μl reverse transcription step) in the reaction. Comparison with standard curves for each subtype (included in each experiment) permitted calculation of absolute values for each sample (transcripts/μg input RNA). In addition, transcripts for a housekeeping gene, APRT, were measured so that values could be expressed relative to this (transcripts/1000 APRT). In a single QPCR experiment, all of the measurements were made in triplicate; the standard curve was also run at least in duplicate in each reaction.

Measurement of Hyaluronan—For all experiments to measure HA, preadipocytes were plated in CM in 6-well plates but then washed in the same medium but without fetal calf serum and incubated in this for the 24 h prior to collection. Culture supernatants from nonmodified preadipocytes (treated or not with db-cAMP or TSHR ligands) and untreated L629F-expressing preadipocytes (48 h in serum-free medium) at 70–100% confluence were collected, centrifuged to remove dead cells, and stored at −80 °C until analysis.

HA was measured in neat 24-h supernatants (determined by preliminary experiments using neat, 1:10 and 1:100) using a commercially available enzyme-linked immunosorbent assay (ELISA; Corgenix) according to the manufacturer's instructions. The results are expressed as the mean ± S.E. ng/10^4 cells.

Western Blotting—Subcutaneous preadipocytes from four individuals were cultured in 60-mm dishes until 70% confluent and treated (or not) for 24 h with 10^{-3} M db-cAMP. The proteins were extracted in Laemmli buffer containing 1 mM sodium orthovanadate and 1 mM phenylmethylsulfonyl fluoride. The samples (containing 20 μg of protein) were separated by 10% SDS-PAGE, and the gel was then electroblotted onto polyvinylidene difluoride membrane as previously described (17). The blots were probed with goat polyclonal antibodies to HAS1 and HAS2 from Santa Cruz (sc-23145 and sc-34067). Both antibodies were used at 1:1000 dilution, and the blots were incubated at 4 °C overnight. The proteins were detected using an anti-goat IgG-horseradish peroxidase conjugate (1:5000, room temperature for 1 h; GE Healthcare) and visualized by enhanced chemiluminescence (ECL Plus; GE Healthcare).

Knockdown of HAS1 and HAS2 Using siRNA—Preadipocytes ($n = 4$) were plated in 60-mm dishes until 70% confluent, and 24 h before transfection they were switched to culture medium without antibiotics. The cells were incubated at 37 °C overnight in 2.5 ml of culture medium containing 5 μl of Lipofectamine 2000 (Invitrogen) and 1 μl of 100 μM HAS1, HAS2, or scrambled siRNA (Applied Biosciences) to produce a final concentration of 40 nM. At the end of the incubation the cells were washed, resuspended in Dulbecco's modified Eagle's medium, and treated for 24 h with 10^{-3} M db-cAMP; RNA and culture supernatants were collected for QPCR and ELISA measurements.

Reporter Assays—Initially HAS1 and HAS2 locus sequences were analyzed for the presence of putative transcription factor-binding sites using the updated MatInspector program from the Genomatix suite (18). The reporter assays employed three plasmids to test cAMP-mediated transactivation of HAS1. The first comprises 201 base pairs of HAS1 proximal promoter and includes the cAMP-responsive element (CRE) recognition sequence (TGACGTCA) at −128/−120; the second is identical, but the CRE has been mutated (tgacTGACGTCA to taacATACCTTA, in this modified promoter Genomatix software did not identify a CREB site, all other sites remained recognizable, and the changes created no new sites); the third comprises the proximal 108 base pairs and thus lacks the CRE. In all cases the promoter regions were cloned into the EcoRI/HindIII site of the pGL3 modified basic luciferase reporter vector as previously described (19). In addition, the pSVβgal (Promega) plasmid was incorporated to control for transfection efficiency. Transcriptional response to cAMP was assessed in several different cell types including A293, COS, and C2C, all plated at 1×10^4 cells/well in 24-well plates in Dulbecco's modified Eagle's medium containing 10% fetal calf serum.

All of the cell types were transfected with 500 ng of luciferase reporter and 100 ng of β-galactosidase reporter using Transfast™ transfection reagent (Promega) according to the manufacturer's instructions. After 24 h in serum-free medium, the cells were treated for 4 or 24 h with 10^{-5} M forskolin ± 10^{-4} M isobutylmethylxanthine or 10^{-4} M dibutyryl cAMP; 24 h later the cells were lysed in 120 μl/well lysis buffer (Promega). To measure β-galactosidase, 50 μl of cell lysate was transferred to a clear 96-well plate and incubated with an equal volume of ice-cold assay buffer (120 mM $Na_2HPO_4 \cdot 12H_2O$, 80 mM NaH_2PO_4, 2 mM $MgCl_2 \cdot 6H_2O$, 100 mM β-mercaptoethanol, 1.33 mg/ml *o*-nitrophenyl-β-D-galactopyranoside, pH 7.5) at room temperature for 30 min, and the absorbance was read at 420 nm using an ELISA plate reader. the results are expressed in optical density units. The luciferase activity in a 50 μl of cell lysate was determined using Promega's dual luciferase reporter assay system according to the manufacturer's instructions and was measured on an automatic luminometer (PerkinElmer Life Sciences; TR717). The results are expressed in relative light units. The final results are expressed as corrected relative light units, *i.e.* normalization of luciferase values to β-galactosidase activity (relative light units/optical density unit). Individual experiments were all performed in triplicate.

Chromatin Immunoprecipitation Assay—Preadipocytes ($n = 3$) were cultured in 100-mm dishes in CM until they reached 80% confluence. They were serum-starved for 24 h and then treated or not for 4 h with 10^{-3} M dibutyryl cAMP. Chromatin was prepared, and ChIP assays were performed using the EpiQuick ChIP kit (Epigentek) according to the manufacturer's instructions. Briefly, the cells were washed with phosphate-buffered saline and then fixed with 1% formaldehyde for 15 min. The cross-linked nuclear extracts were sonicated to obtain small length DNA fragments ranging from 200 to 800 bp. A polyclonal antibody to CREB (sc-186x; Santa Cruz) was used for the immunoprecipitation. The human HAS1 promoter CRE site (−128/−120) was analyzed by PCR amplification; the following primers were used: HAS-1F (76-bp fragment immediately adjacent to CRE), CCCGCCTGCGCTGGTCTTCA; and HAS-1R, CTCTCCGGCTTGCTCTCC. The human HAS2 promoter (−664/−656) full site CRE was analyzed using the following primers: HAS-2F (113-bp fragment spanning CRE), ACGGCAGAAACCTCTTTATGA; and HAS-2R, TCTAAAAAGATCGCGGTGGT.

Statistical Analysis—The data were analyzed using the Bayesian *t* test with false detection rate correction, Wilcoxon signed ranks test, or Student's *t* test. In all cases $p < 0.05$ was considered significant. The statistical analysis applied is indicated in the table/figure legends.

RESULTS

Gene Induction by Activating TSHR—To investigate a possible role for TSHR activation in the lineage-specific differentiation of adipose-derived precursors, we compared the gene expression profiles (Fig. 1) of control (empty vector) subcutaneous preadipocytes from four individuals with the same populations expressing L629F TSHR. After applying stringent statistical methods (Bayesian *t* test with false detection rate correction) to account for the high degree of intrasample variation, only 48 genes remained whose expression was significantly different between the two. HAS1 and HAS2 were among the 27 genes whose expression was significantly up-regulated (3.3- and 1.5-fold, respectively) in the L629F populations.

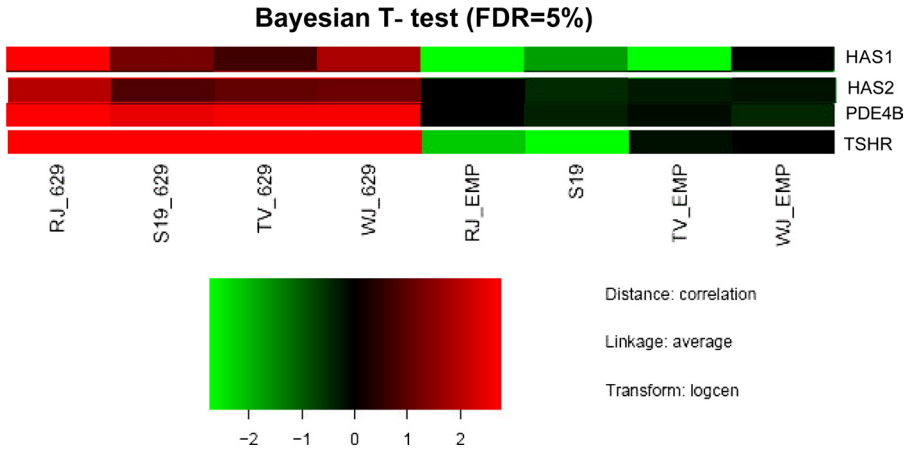

FIGURE 1. **A heat map representation of selected genes whose expression was significantly increased (Bayesian *t* test, false detection rate (*FDR*) correction) in subcutaneous preadipocytes expressing activating mutant TSHR L629F compared with empty vector controls (*EMP*).** *PDE4B*, phosphodiesterase type 4B.

TABLE 2

Comparison (Wilcoxon) of HAS isoform transcript levels and HA in the culture medium in preadipocytes ($n = 10$) from various fat depots (predominantly subcutaneous), either control or expressing activating mutant TSHR (L629F)

HAS1 and HAS2 TCN are expressed per 1000 copies of the housekeeping gene. HA is expressed as ng/10^4 cells. The results are the means ± S.E. of all samples analyzed in the group, with each individual sample being measured in triplicate.

	Control	L629F	*p* value
HAS1 TCN	21.2 ± 7.5	57.7 ± 22.9	$p < 0.02$
HAS2 TCN	226 ± 84.2	356 ± 134	$p < 0.04$
HA ng/10^4 cells	657 ± 174	931 ± 135	$p < 0.03$

Activating TSHR Induces HAS1/2 Transcripts and HA Production—To confirm the array data, a further 10 preadipocyte samples (predominantly subcutaneous) were then analyzed using QPCR for HAS isoform transcript measurement and ELISA to quantify HA production. The results are summarized in Table 2. In all of the samples analyzed, the APRT housekeeper "crossing the threshold" (C_t) values were in the region of 20–21. HAS1 C_t values were much higher (27–31), indicating the low transcript levels, and HAS2 transcripts were ~10-fold more abundant than HAS1 (C_t values in the range 23–27).

HAS1 and HAS2 TCN and HA in the culture medium were significantly increased in preadipocytes expressing L629F TSHR when compared with control. Because no significant differences were observed between nonmodified preadipocytes or the same cells transduced with the empty vector (data not shown), both populations provided adequate controls.

HAS Transcription and HA Production Are Induced Using Agents to Increase cAMP—Activation of the TSHR, as in the L629F expressing cells, induces signaling via the cAMP cascade. Consequently we used db-cAMP to investigate whether the observed increases were indeed caused by elevated cAMP; the results are shown in Fig. 2.

Treatment of nonmodified preadipocytes with 10^{-3} M db-cAMP ($n = 8$) for 4 h significantly increased HAS1 TCN ($p < 0.02$) and HAS2 TCN ($p < 0.008$). When treatment was for 24 h, there were significant increases in HAS1 TCN ($p < 0.05$), HAS2 TCN ($p < 0.008$), and HA by ELISA ($p < 0.0001$). HAS3 TCN were not significantly modified by the treatment (data not shown).

To determine whether the db-cAMP treatment had induced an equivalent increase in HAS1 and HAS2 proteins in the preadipocytes, Western blot analysis was attempted. When probing with an antibody to HAS1, the protein bands corresponding to the expected M_r were at the limit of detection and impossible to quantify. The HAS2 antibody produced a strong signal with a protein of apparent molecular mass 53 kDa, and densitometry, used to produce a ratio of HAS2 (53 kDa):actin ($n = 4$), revealed that its expression was increased from 7.6 ± 0.35 to 9.6 ± 0.98 ($p < 0.03$, Student's) by treatment with the cAMP mimetic. A protein at 63 kDa was also increased by db-cAMP but was at the limit of detection. A representative blot is shown in Fig. 3.

Treatment with siRNA Reverses the db-cAMP-induced Increase in HA Production—In view of the lack of protein expression data for HAS1, we then applied HAS1 siRNA to subcutaneous preadipocytes from four individuals. In basal conditions, 40 nM HAS1 siRNA produced a 58% reduction in transcripts for HAS1 ($p < 0.03$), a 52% increase in HAS2 ($p < 0.04$), and no change in secreted HA (Fig. 4*A*). When the cells were stimulated with 10^{-3} M db-cAMP, HAS1 siRNA produced an 80% reduction in transcripts for HAS1 ($p < 0.0005$), no change in HAS2, and a 49% reduction in HA ($p < 0.007$) in the culture medium (Fig. 4*B*).

Equivalent experiments using HAS2 siRNA produced a 56% reduction in transcripts for HAS2, a 60% increase in HAS1 transcripts, and a 70% reduction in secreted HA (all $p < 0.05$) in basal conditions (Fig. 4*C*). In db-cAMP stimulated cells HAS2 siRNA resulted in a 61% decrease in HAS2 transcripts accompanied by a 38% reduction in secreted HA (both $p < 0.05$) but did not affect HAS1 transcript levels (Fig. 4*D*).

Do the HAS1 or HAS2 Promoters Contain a Functional CRE?—The proximal promoter of HAS1 (a tata-less gene) has a perfect full site consensus CRE (TGACGTCA) at position −128/−120 relative to the transcription start site; there are also two half-sites further upstream. The HAS2 promoter also contains a full site CRE at −656 (and half-sites at −892, −2751 and −5305) relative to the transcription start site, but unlike the full CRE in the HAS1 promoter, this is not predicted to be functional (20).

Thus We Performed Reporter Assays to Investigate the HAS1 Promoter CRE Further—Preliminary experiments used a reporter construct in which luciferase is under the control of the proximal 201 bp of HAS1 promoter, containing the intact CRE, which was transfected into four different cell types (COS, HepG2, C2C, and A293). The only cell type to produce any increase in light output when treated with db-cAMP or forskolin was the A293. Consequently they were selected for further study.

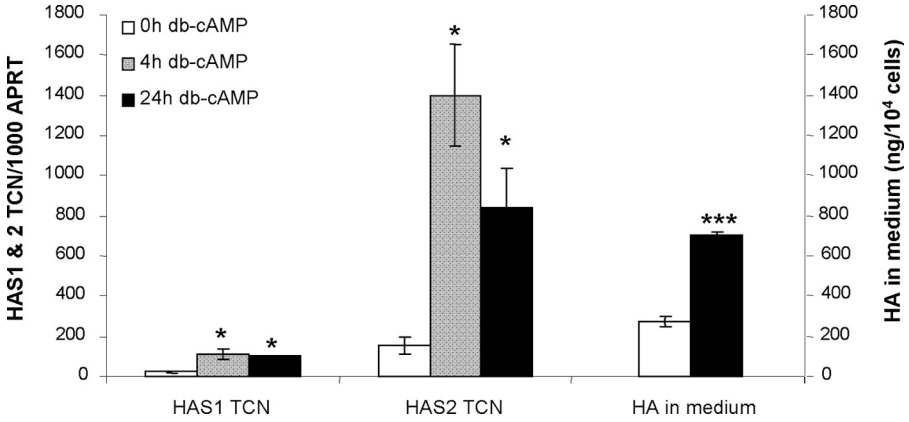

FIGURE 2. **HAS1 and HAS2 transcript levels (expressed per 1000 copies of the APRT housekeeper gene) and HA secreted into the medium (reported as ng/10^4 cells) are both the means ± S. E. in preadipocytes ($n = 8$) untreated (0 h) or following 4 or 24 h of treatment with 10^{-3} M db-cAMP.** *, $p < 0.05$; ***, $p < 0.0005$ (Student's).

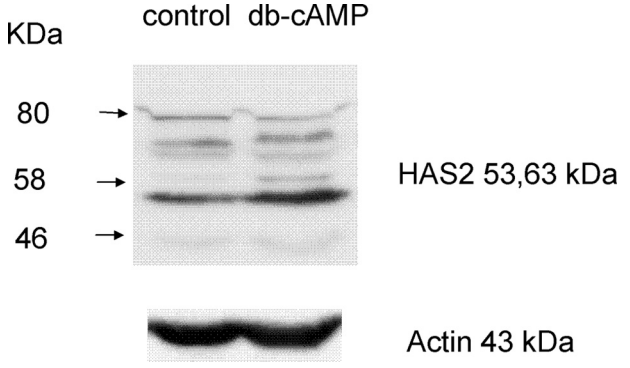

FIGURE 3. **Western blot analysis of HAS2 expression in preadipocytes treated (cAMP) or not (control) with 10^{-3} M db-cAMP for 24 h.** The blots were stripped and reprobed with actin to demonstrate equal loading and provide a reference point for densitometry measurements.

Subsequent experiments employed the same construct in addition to several controls; these were the empty pGL3 vector, the proximal HAS1 promoter from −108 (lacks the CRE), and the proximal HAS1 promoter from −201 in which the CRE had been mutated by site-directed mutagenesis. A representative experiment shown in Fig. 5 illustrates two points: 1) that significant increases in light output were observed only in the presence of an intact CRE and a cAMP mimetic and 2) that the −201 promoter containing an intact CRE contains elements necessary for basal transcription of the HAS1 gene. A similar 2–3-fold increase in light output was obtained using 10^{-5} M forskolin, but again only in A293 cells transfected with the construct in which the CRE was intact (data not shown).

To determine whether the CRE is functional *in vivo*, we then undertook chromatin immunoprecipitation experiments on preadipocytes treated for 4 h with 10^{-3} M db-cAMP, using an antibody to CRE binding protein, CREB. Subsequent amplification (QPCR) of the HAS1 promoter CRE region using primers immediately adjacent to the CRE (amplicon size 76bp) produced a relative fold increase of 3.3 ± 0.8 ($n = 3$). In contrast, no PCR products were detected when using the primer pair designed to produce a larger amplicon (287 bp) flanking the CRE. Fig. 6*A* shows a representative example of the 76-bp amplicons obtained. For completeness we also examined the HAS2 promoter. There was a relative fold increase of 2.6 ± 0.9 ($n = 3$) when using a primer pair that covers the −664/−656 full site CRE. The primers produced an amplicon of 113 bp, as illustrated in Fig. 6*B*. No consistent PCR products were obtained using primer pairs just upstream of the −664/−656 full site or in the region of the intronic CRE or −5305, −2754, and −892 half-site CREs in the HAS2 promoter.

TSHR Ligands Have Varying Effects on HAS Isoform Transcription and HA Production—The experiments performed thus far have either introduced constitutively active TSHR or biochemical reagents to increase intracellular cAMP, both of which target the entire preadipocyte population. To mimic the *in vivo* situation existing in patients with thyroid dysfunction, in which a small proportion of cells express the TSHR, we investigated the effects of physiological (TSH) and pathological (TSAB) TSHR ligands in subcutaneous preadipocytes from seven individuals. The results are summarized in Table 3; small but significant increases in HA were induced by TSH (12%, $p < 0.001$) and a monoclonal TSAB (9% $p < 0.04$). A similar low level stimulation (14% $p < 0.05$) was obtained with a TSHR antibody (3G4) devoid of biological activity, although BA8, a TSHR antibody that also lacks bioactivity, produced no significant change in HA production. The possibility that the TSHR antibodies might be exerting an effect by interacting via their Fc region was also eliminated by the lack of response to an unrelated monoclonal antibody to thyroid peroxidase (data not shown).

Are There Adipose Depot-specific Differences in the Regulation of HAS1 and HAS2 by cAMP?—An adipose depot of particular significance in hyperthyroid patients is the orbit, in which overproduction of HA is a major contributor to the tissue remodeling, which occurs in GO. Preliminary experiments, using semi-quantitative PCR supported by metabolic labeling and chromatography, demonstrated an approximate doubling of secreted and cell-associated HA across the size spectrum in GO orbital preadipocytes expressing a constitutively active TSHR when compared with empty vector or wild type TSHR-expressing controls (data not shown).

Subsequently we performed a range of experiments on orbital preadipocytes, mainly from GO patients. Analysis of six further individuals (five GO and one normal) revealed that HA in the culture medium was significantly increased in the L629F TSHR-expressing cells when compared with control, as shown in Table 4.

When treated with db-cAMP (three GO and one normal) HAS1 and HAS2 transcripts (measured by QPCR, a similar 10-fold abundance of HAS2 compared with HAS1 was observed) were significantly increased at 4 and 24 h ($p < 0.05$) and HA measured in the culture supernatant at 24 h was increased, but the difference did not reach significance (Table 4).

The response of orbital preadipocytes to TSH and TSAB was more complex and is summarized in Table 4. No significant response was obtained with either ligand in preadipocytes from six GO and three normal orbits (data not shown). However, when analyzing the results of the GO and normal preadipocytes separately, we observed 18 and 24% increases in secreted HA in response to TSAB ($p < 0.05$) and TSH ($p < 0.06$), respectively, in the normal samples. In contrast, there was no significant difference in HA in the culture medium of preadipocytes from GO orbits ($n = 6$) incubated with either ligand. Furthermore, there was a significant difference ($p < 0.05$) in the HA secreted response to TSH and TSAB of normal and GO orbital preadipocytes.

DISCUSSION

Our microarray data, demonstrating a significant up-regulation in HAS1 and HAS2 mRNA in preadipocytes expressing a gain-of-function TSHR, indicate a role for TSHR activation in regulating HA production. This is clinically relevant, because patients across the spectrum of thyroid dysfunction demonstrate alterations in the quality and quantity of GAG present in their skin. In both hyper- and hypothyroidism, the predominant GAG is HA, leading to accumulation of mucin deposits in the dermis and subcutaneous tissues (21). The condition is generalized in hypothyroidism but localized, mainly to the pretibial region and orbit, in hyperthyroid GD. The histological changes are similar in the two conditions and in hypothyroidism respond swiftly to thyroxine treatment (22), leading to the suggestion that reduced thyroid hormone rather than TSH excess is responsible.

Smith *et al.* (23) demonstrated that thyroid hormones exert a negative effect on GAG synthesis in human skin fibroblasts *in vitro* and support earlier *in vivo* studies in rodents (24) and humans (25). A role for thyroid hormone in stimu-

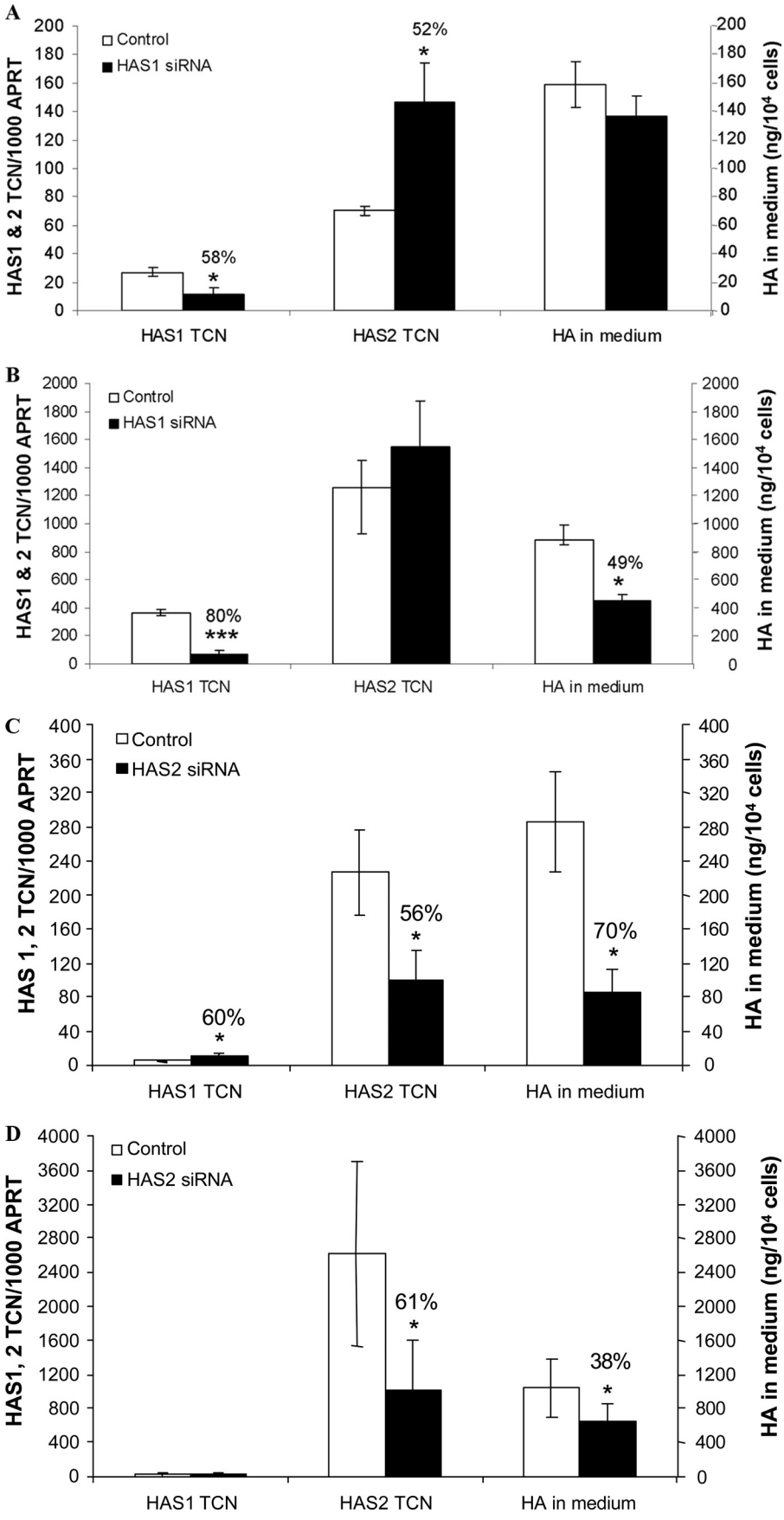

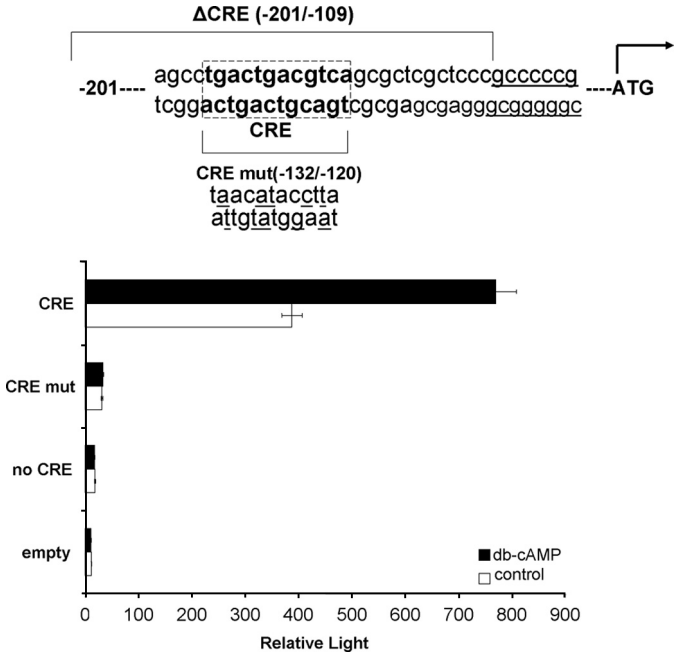

FIGURE 5. **Reporter assay in which A293 cells were transfected with the luciferase constructs driven by the HAS1 proximal promoter containing the CRE (*CRE*), lacking the CRE (*no CRE*), and having a mutated form of CRE (*CRE mut*, mutated residues underlined).** The cells were treated or not with 10^{-3} M db-cAMP. The results are expressed as relative light units, *i.e.* the ratio of light output:β-galactosidase activity.

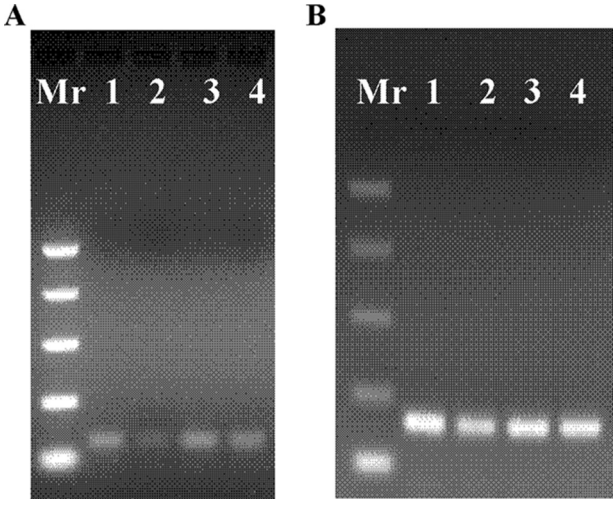

FIGURE 6. **Agarose gel (2%) electrophoresis of HAS1 promoter CRE region PCR amplicons (76 bp) (*A*) and HAS2 promoter CRE region PCR amplicons (113 bp) (*B*) obtained using (in both *A* and *B*) input chromatin (*lanes 1* and *3*) and ChIP (*lanes 2* and *4*).** *Lanes 1* and *2*, no db-cAMP; *lanes 3* and *4*, with 10^{-3} M db-cAMP.

lating HA breakdown has also been suggested (21), although reports are contradictory (26, 27).

For thyroid hormones to impact gene expression, the relevant promoters must contain a TRE; we have identified an imperfect DR4 ~1.9 kb from the transcriptional start site and an ER6 half-site just upstream from the CRE in the HAS1 promoter; and the HAS2 promoter contains three half-sites. However, the absence of thyroid hormone inhibition of HAS expression cannot explain the skin changes in GD, and thyroxine replacement, in addition to raising circulating T4, will also lower TSH. Furthermore, one of us has previously reported the presence of TSHR transcripts and immunostaining in various adipose tissues and pretibial skin (28, 29). Thus we have confirmed our microarray data and extended the investigations further using preadipocyte fibroblasts from orbital and subcutaneous fat. Preadipocytes from all sites induced to express constitutively active TSHR had higher levels of HAS1 and HAS2 TCN, leading to increased HA in the culture medium, when compared with their nonmodified counterparts. We are aware that the introduction of constitutively active TSHR mutants into the preadipocytes has the disadvantage that all cells will express the receptor and hence experience increased intracellular cAMP levels. Although it can indicate the likely impact of signaling via the TSHR on processes such as, for example, adipogenesis or production of extracellular matrix, it does not accurately replicate the *in vivo* situation in which far fewer preadipocyte fibroblasts express the receptor.

In previous studies (28) we reported that 1–5% of freshly isolated preadipocytes (orbital and subcutaneous) express the TSHR when assessed using immunocytochemistry. All of our current experiments were conducted using low passage cells, and we have confirmed the presence of TSHR transcripts in all

TABLE 3

HA secreted into the medium

The values shown are from preadipocytes ($n = 7$) untreated or treated for 9 days with 5 milliunits/ml TSH, a monoclonal thyroid-stimulating antibody (IriSab), or monoclonal antibodies to the TSHR devoid of biological activity, 3G4 and BA8 (Student's). The values are reported as ng/10^4 cells (means ± S.E.).

	HA ng/10^4 cells (means ± S.E.)	*p* value	Percentage control
Untreated	252 ± 59		100
5 milliunits/ml TSH	270 ± 57	$p < 0.001$	112 ± 0.03
TSAB mAb IriSab	263 ± 56	$p < 0.04$	109 ± 0.03
TSHR mAb 3G4	276 ± 59	$p < 0.05$	114 ± 0.05
TSHR mAb BA8	252 ± 54	NS	100 ± 0.05

TABLE 4

HA secreted into the medium

The values shown are from preadipocytes from orbital samples in response to expression of activating mutant TSHR (L629F); following 24 h of treatment with 10^{-3} M db-cAMP (db-cAMP); following treatment for 9 days with 5 milliunits/ml TSH, or a monoclonal thyroid stimulating antibody (TSAB). NS, not significant. The values are reported as ng/10^4 cells (means ± S.E.).

	Control	Stimulated	*p* value
Normal and GO combined			
L629F TSHR, $n = 6$	425 ± 100	528 ± 107	$p < 0.05$ (Wilcoxon)
db-cAMP, $n = 4$	113 ± 16	165 ± 26	$p < 0.08$ (Student's)
Normal and GO separately			
TSAB, normal $n = 3$	318 ± 103	377 ± 123	$p < 0.05$ (Student's)
TSH, normal $n = 3$	318 ± 103	395 ± 135	$p < 0.06$ (Student's)
TSAB, GO $n = 6$	417 ± 93	317 ± 106	NS (Student's)[a]
TSH, GO $n = 6$	417 ± 93	317 ± 110	NS (Student's)[a]

[a] Response of GO preadipocytes to both ligands significantly lower than that of normal preadipocytes ($p < 0.05$).

FIGURE 4. **Effect of 40 nM HAS1 or HAS2 siRNA on HAS1 and HAS2 transcript levels (expressed per 1000 copies of the APRT housekeeper gene) and HA secreted into the medium (reported as ng/10^4 cells) are both the means ± S. E. in preadipocytes ($n = 4$).** *A*, HAS1 siRNA in basal conditions. *B*, HAS1 siRNA cells stimulated for 24 h with 10^{-3} M db-cAMP. *C*, HAS2 siRNA in basal conditions. *D*, HAS2 siRNA cells stimulated for 24 h with 10^{-3} M db-cAMP. *, $p < 0.05$; **, $p < 0.005$; ***, $p < 0.0005$ (Student's).

of them using QPCR (data not shown). The increase in HA induced by TSHR ligands was more modest than that obtained in the activating TSHR-expressing cells (9–24% *versus* 24–42%). Given the expected difference in the proportion of cells expressing the TSHR in the two conditions, one might have expected a larger differential.

In previous studies examining the transforming growth factor β1-dependent differentiation of fibroblasts to myofibroblasts we have identified a central involvement of increases in extracellular and pericellular HA, whether this results from increased HA synthesis (6, 30) or decreased HA turnover (19). This HA accumulation is essential but not sufficient on its own for differentiation to occur. It is not yet clear whether the same HA dependence will be a feature of phenotypic changes induced by the mechanisms described here, and this will be the subject of future studies.

The level of HA increase we obtained with bovine TSH is similar to that previously reported by one of us for dermal fibroblasts, although in the earlier study recombinant human TSH failed to elicit a response (31). Similarly Smith and Hoa (11) examined orbital fibroblasts from a single GO patient; TSH did not increase HA generation. A later study from the same group reported no increase in HA production by human thyrocytes in response to recombinant TSH (32), although their findings are at variance with those of several other authors who observed increased synthesis of HA in pig or rat thyroid cells in response to the hormone (33, 34). There are differences between the studies using nonthyroidal cells that merit comment. We have used preadipocyte fibroblasts of low passage number from adipose tissue, in contrast to dermal or orbital fibroblasts of unspecified passage number. Although we have not examined the effect of recombinant TSH, the similar level of HA increase induced by a second TSHR agonist, a monoclonal TSAB, adds significant weight to the finding. Although previous workers have found no effect of serum immunoglobulins from GD patients on fibroblast HA production (35), we are unaware of any studies that have examined the effect of a monoclonal TSAB.

We were surprised to observe that a TSHR monoclonal antibody devoid of bioactivity, 3G4 (recognizes a linear epitope in the N terminus of the extracellular ligand-binding domain of the receptor) (34), was also able to induce HA production. The result suggests an alternative signal transduction pathway consequent to TSHR cross-linking. A simple interaction between the Fc region of the monoclonal antibody with the Fc receptor was eliminated by the absence of HA increase when the cells were incubated with other nonagonist monoclonal antibodies such as BA8 (recognizes the TSHR three-dimensional conformation) (36) and mAb 47 (binds a linear epitope in thyroid peroxidase) (37).

The responses of normal and GO orbital preadipocyte fibroblasts differed. All GO patients will have received previous treatment with corticosteroids, and thus the most active components, *e.g.* TSHR-expressing cells, may already have been depleted. This could explain the difference in response to TSH and the monoclonal TSAB reported here and the absence of response reported by others (11). Furthermore, orbital preadipocyte fibroblasts are distinct as illustrated by their reduced responsiveness to the T3-induced inhibition of GAG accumulation *in vitro* when compared with cells from the skin (38).

The relevance of the main TSHR signaling cascade to the process is illustrated by the robust increase in HA in the culture medium and in HAS1 and 2 TCN obtained when cells were treated with the cAMP mimetic, db-cAMP. Our results confirm two earlier studies; Tomida *et al.* (39) reported that cAMP increases HA activity in rat fibroblasts *in vitro* and in the rat thyroid cell line FRTL5 TSH stimulated GAG synthesis, with the effect being reproduced by db-cAMP (34). This led us to investigate the proximal promoters of the HAS1 and HAS2 genes. Both contain full site CREs, but only the former is predicted to be active, because it is located within the first 200 bp from the transcriptional start site (40). The first point of note was that the −201 construct (which contains the CRE) appears to comprise a minimal promoter, because it produced an ~10-fold increase in light output, compared with the empty vector, in all four cell types. In contrast, it was only in the A293 cells that we were able to observe a clear increase in light output in response to db-cAMP and forskolin. Both agents induced a 2–4-fold increase in light output, and this was restricted to the construct containing the intact CRE. The HAS1 gene promoter lacks a tata box. Previous workers have identified HAS1 as a potential target for regulation by cAMP. They undertook functional measurements of several other target genes (excluding HAS1) described as tata-less and found that all responded to cAMP with a 2–4-fold increase in transcriptional activity (20). The results we obtained are in keeping with this finding and suggest that HAS1 transcription is indeed regulated by the cAMP-dependent protein kinase pathway, and the results of our ChIP assays illustrate that it has *in vivo* relevance. The same method indicates that the HAS2 promoter full site CRE is also functional.

In conclusion, in addition to the well documented negative effect of thyroid hormone, our results indicate that "pathological" TSHR activation plays a role in regulating production of the extracellular matrix component HA by preadipocyte fibroblasts isolated from various fat depots. By pathological we refer to the receptor activation occurring in GD patients in response to TSAB or in hypothyroid patients with compensatory elevated TSH. The mechanism is likely to be of less importance in healthy euthyroid individuals. The study may provide an explanation for the disordered production of HA occurring in patients with thyroid dysfunction that leads to widespread myxoedema or localized HA accumulation, features of hypothyroidism and hyperthyroid GD, respectively.

Acknowledgments—We greatly appreciate the gift of monoclonal antibodies (IRISAB2, BA8, and 3G4) from Dr. Sabine Costagliola (Institut de Recherche Interdisciplinaire en Biologie Humaine et Moleculaire, Brussels, Belgium) and of mAb 47 from Dr. Pierre Caryon (INSERM U555, Marseille, France). The continued support of Professors Maurice Scanlon and Aled Phillips is gratefully acknowledged.

REFERENCES

1. Vassart, G., and Dumont, J. E. (1992) *Endocr. Rev.* **13,** 596–611
2. Crisp, M. S., Lane, C., Halliwell, M., Wynford-Thomas, D., and Ludgate, M. (1997) *J. Clin. Endocrinol. Metab.* **82,** 2003–2005

3. Abe, E., Marians, R. C., Yu, W., Wu, X. B., Ando, T., Li, Y., Iqbal, J., Eldeiry, L., Rajendren, G., Blair, H. C., Davies, T. F., and Zaidi, M. (2003) *Cell* **115,** 151–162
4. Turley, E. A., Noble, P. W., and Bourguignon, L. Y. (2002) *J. Biol. Chem.* **277,** 4589–4592
5. Itano, N., Sawai, T., Yoshida, M., Lenas, P., Yamada, Y., Imagawa, M., Shinomura, T., Hamaguchi, M., Yoshida, Y., Ohnuki, Y., Miyauchi, S., Spicer, A. P., McDonald, J. A., and Kimata, K. (1999) *J. Biol. Chem.* **274,** 25085–25092
6. Meran, S., Thomas, D., Stephens, P., Martin, J., Bowen, T., Phillips, A., and Steadman, R. (2007) *J. Biol. Chem.* **282,** 25687–25697
7. Smith, T. J., Bahn, R. S., and Gorman, C. A. (1989) *Endocr. Rev.* **10,** 366–391
8. Weetman, A. P. (1993) *Q. J. Med.* **86**, 473–477
9. Kaback, L. A., and Smith, T. J. (1999) *J. Clin. Endocrinol. Metab.* **84,** 4079–4084
10. Wang, H. S., Tung, W. H., Tang, K. T., Wong, Y. K., Huang, G. J., Wu, J. C., Guo, Y. J., and Chen, C. C. (2005) *J. Cell. Biochem.* **95,** 256–267
11. Smith, T. J., and Hoa, N. (2004) *J. Clin. Endocrinol. Metab.* **89,** 5076–5080
12. Paschke, R., and Ludgate, M. (1997) *N. Engl. J. Med.* **337,** 1675–1681
13. Zhang, L., Baker, G., Janus, D., Paddon, C., Fuhrer, D., and Ludgate, M. (2006) *Invest. Opthalmol. Vis. Sci.* **47,** 5197–5203
14. Fuhrer, D., Lewis, M. D., Alkhafaji, F., Starkey, K., Paschke, R., Wynford-Thomas, D., Eggo, M., and Ludgate, M. (2006) *Endocrinology* **144,** 4018–4030
15. Baldi, P., and Long, A. D. (2001) *Bioinformatics* **17,** 509–519
16. Benjamini, Y., and Hochberg, Y. (1995) *J. R. Stat. Soc.* **57,** 289–300
17. Al-Khafaji, F., Wiltshire, M., Fuhrer, D., Mazziotti, G., Lewis, M. D., Smith, P. J., and Ludgate, M. (2005) *J. Mol. Endocrinol.* **34,** 209–220
18. Cartharius, K., Frech, K., Grote, K., Klocke, B., Haltmeier, M., Klingenhoff, A., Frisch, M., Bayerlein, M., and Werner, T. (2005) *Bioinformatics* **21,** 2933–2942
19. Jenkins, R. H., Thomas, G. J., Williams, J. D., and Steadman, R. (2004) *J. Biol. Chem.* **279,** 41453–41460
20. Conkright, M. D., Guzmán, E., Flechner, L., Su, A. I., Hogenesch, J. B., and Montminy, M. (2003) *Mol. Cell* **11,** 1101–1108
21. Gabrilove, J. L., and Ludwig, A. W. (1957) *J. Clin. Endocrinol. Metab.* **17,** 925–932
22. Gabrilove, J. L., Alvarez, A. S., and Churg, J. (1960) *J. Clin. Endocrinol. Metab.* **20,** 825–832
23. Smith, T. J., Murata, Y., Horwitz, A. L., Philipson, L., and Refetoff, S. (1982) *J. Clin. Invest.* **70,** 1066–1073
24. Schiller, S., Slover, G. A., and Dorfman, A. (1962) *Biochim. Biophys. Acta* **58,** 27–33
25. Lund, P., Hørslev-Petersen, K., Helin, P., and Parving, H. H. (1986) *Acta Endocrinol.* **113,** 56–58
26. Arbogast, B., Hopwood, J. J., and Dorfman, A. (1975) *Biochem. Biophys. Res. Commun.* **67,** 376–382
27. Stair-Nawy, S., Csóka, A. B., and Stern, R. (1999) *Biochem. Biophys. Res. Commun.* **266,** 268–273
28. Crisp, M., Starkey, K. J., Lane, C., Ham, J., and Ludgate, M. (2000) *Invest. Opthalmol. Vis. Sci.* **41,** 3249–3255
29. Daumerie, C., Ludgate, M., Costagliola, S., and Many, M. C. (2002) *Eur. J. Endocrinol.* **146,** 35–38
30. Webber, J., Jenkins, R. H., Meran, S., Phillips, A., and Steadman, R. (2009) *Am J. Pathol.* **175,** 148–160
31. Paschke, R., Metcalfe, A., Alcalde, L., Vassart, G., Weetman, A., and Ludgate, M. (1994) *J. Clin. Endocrinol. Metab.* **79,** 1234–1238
32. Gianoukakis, A. G., Jennings, T. A., King, C. S., Sheehan, C. E., Hoa, N., Heldin, P., and Smith, T. J. (2007) *Endocrinology* **148,** 54–62
33. Wegrowski, J., Bellon, G., Haye, B., and Borel, J. P. (1989) *Cell Biol. Int. Rep.* **13,** 881–890
34. Shishiba, Y., Yanagishita, M., Hascall, V. C., Takeuchi, Y., and Yokoi, N. (1988) *J. Biol. Chem.* **263,** 1745–1754
35. Metcalfe, R. A., Davies, R., and Weetman, A. P. (1993) *Thyroid* **3,** 207–212
36. Costagliola, S., Rodien, P., Many, M. C., Ludgate, M., and Vassart, G. (1998) *J. Immunol.* **160,** 1458–1465
37. Finke, R., Seto, P., Ruf, J., Carayon, P., and Rapoport, B. (1991) *J. Clin. Endocrinol. Metab.* **73,** 919–921
38. Smith, T. J., Bahn, R. S., and Gorman, C. A. (1989) *J. Clin. Endocrinol. Metab.* **69,** 1019–1023
39. Tomida, M., Koyama, H., and Ono, T. (1977) *Biochem. J.* **162,** 539–543
40. Tinti, C., Yang, C., Seo, H., Conti, B., Kim, C., Joh, T. H., and Kim, K. S. (1997) *J. Biol. Chem.* **272,** 19158–19164